Article:
Wiedeking, M., Krtička, M., Bernstein, L. A. et al. (18 more authors) (2016) γ-ray decay from neutron-bound and unbound states in Mo 95 and a novel technique for spin determination. Physical Review C. 024303. pp. 1-11. ISSN 2469-9993

https://doi.org/10.1103/PhysRevC.93.024303

γ-ray decay from neutron-bound and unbound states in ^{95}Mo and a novel technique for spin determination

M. Wiedeking,[1,*] M. Krtička,[2] L. A. Bernstein,[3,4] J. M. Allmond,[5,6] M. S. Basunia,[7] D. L. Bleuel,[3] J. T. Burke,[3] B. H. Daub,[4,8] P. Fallon,[7] R. B. Firestone,[4,7] B. L. Goldblum,[4] R. Hatarik,[3] P. T. Lake,[7] A. C. Larsen,[9] I.-Y. Lee,[7] S. R. Lesher,[3,10] S. Paschalis,[7] M. Petri,[7] L. Phair,[7] N. D. Scielzo,[3] and A. Volya[11]

[1]*Department of Nuclear Physics, iThemba LABS, P.O. Box 722, 7129 Somerset West, South Africa*
[2]*Faculty of Mathematics and Physics, Charles University, V Holešovičkách 2, 18000 Prague 8, Czech Republic*
[3]*Physical and Life Sciences Directorate, Lawrence Livermore National Laboratory, Livermore, California 94551, USA*
[4]*Department of Nuclear Engineering, University of California, Berkeley, California 94720, USA*
[5]*Department of Physics, University of Richmond, Richmond, Virginia 23173, USA*
[6]*Physics Division, Oak Ridge National Laboratory, Oak Ridge, Tennessee 37831, USA*
[7]*Nuclear Science Division, Lawrence Berkeley National Laboratory, Berkeley, California 94720, USA*
[8]*Weapons and Complex Integration Directorate, Lawrence Livermore National Laboratory, Livermore, California 94551, USA*
[9]*Department of Physics, University of Oslo, 0316 Oslo, Norway*
[10]*Department of Physics, University of Wisconsin-La Crosse, La Crosse, Wisconsin 54601, USA*
[11]*Department of Physics, Florida State University, Tallahassee, Florida 32306, USA*

(Received 21 October 2015; revised manuscript received 14 December 2015; published 1 February 2016)

The emission of γ rays from neutron-bound and neutron-unbound states in ^{95}Mo, populated in the ^{94}Mo(d,p) reaction, has been investigated. Charged particles and γ radiation were detected with arrays of annular silicon and Clover-type high-purity Germanium detectors, respectively. Utilizing p-γ and p-γ-γ coincidences, the ^{95}Mo level scheme was greatly enhanced with 102 new transitions and 43 new states. It agrees well with shell model calculations for excitation energies below $\approx$2 MeV. From p-γ coincidence data, a new method for the determination of spins of discrete levels is proposed. The method exploits the suppression of high-angular momentum neutron emission from levels with high spins populated in the (d,p) reaction above the neutron separation energy. Spins for almost all ^{95}Mo levels below 2 MeV (and for a few levels above) have been determined with this method.

DOI: 10.1103/PhysRevC.93.024303

I. INTRODUCTION

Nuclei that have been studied extensively with previous-generation detector systems can yield a surprising wealth of new information when investigated with modern arrays. This is not limited to work at radioactive ion beam facilities but applies also to studies of nuclei along the valley of β stability. In addition to serving as important benchmarks for nuclear structure theory, the best possible knowledge of the discrete level structure and its associated decay patterns improves the predictability of statistical γ-decay model calculations. These simulations use available information on low-lying levels in the region of low excitation energies (typically below $\approx 2\Delta$, where Δ is the pair-gap parameter) where statistical approaches fail due to low-level densities.

The competition between neutron and γ-ray emission of neutron unbound states not only provides interesting insight into nuclear structure effects, but also has important implications for (n,γ) reaction rates. These rates are fundamental ingredients for calculations of elemental nucleosynthesis [1], advanced fuel cycles [2], and nuclear-waste transmutation [3].

The ratio of the emission probabilities for states above the neutron separation energy S_n is dominated by the probability of neutron emission (characterized by the neutron width Γ_n). This probability can be significantly suppressed if the neutron has to carry high orbital momentum, while at the same time a mismatch of available spin states in the A-n system exists [4]. The suppression of neutron emission has been observed in neutron beam experiments [5], as well as in β-delayed neutron emission studies [6–8]. More recently, this effect has also been reported in measurements using the surrogate method [9–12], and in studies of radioactive ion beam implantations with Clover-type γ-ray detection [13,14] and a total absorption spectrometer [15].

Nevertheless, according to our knowledge this suppression of neutron emission has never been suggested to be used for the determination of spins of discrete levels in nuclei. In this paper, we present ^{94}Mo$(d,p\gamma)$ data that allow for a determination of spins in ^{95}Mo from an analysis of this suppression. Specifically, we exploit the dependence of the ratio of γ-ray decay probability (characterized by the total radiation width Γ_γ) and $\Gamma_n+\Gamma_\gamma$, as a function of spin for states above S_n, and propose a novel method for assigning spins to low-lying levels.

The same set of experimental data has already been used to obtain results related to photon-strength functions in ^{95}Mo [16], and to extract (n,γ) cross sections from the surrogate approach [17]. In Secs. II and III the experimental approach and data analysis are outlined, respectively. Results related to the level and decay scheme, as well as the novel

*wiedeking@tlabs.ac.za

method for spin determination, are presented and discussed in Sec. IV. The main results are then summarized in the last section.

II. EXPERIMENTAL PROCEDURE

The measurement was carried out at the 88-Inch Cyclotron of the Lawrence Berkeley National Laboratory, with ^{95}Mo nuclei populated in the ^{94}Mo$(d,p\gamma)$ reaction at a beam energy of 11 MeV. The average beam current during the 3 day experiment was ∼5.5 nA. The ^{94}Mo target thickness was 250(6) μg/cm^2, as determined from energy loss measurements of ^{226}Ra α particles.

The STARS-LIBERACE detector array [18], consisting of bismuth germanate (BGO) Compton-suppressed Clover-type detectors [19,20] and annular silicon detectors of S2 type [21], was used to detect γ radiation and charged particles from the reaction, respectively. Two clover detectors were placed at 40°, one at 90°, and two at 140° relative to the beam direction, at a distance of 20 cm from the target. Hevimet shields were mounted on each BGO detector to suppress false vetoes from high-multiplicity events. Two identical particle telescopes were mounted upstream and downstream of the target with 150-μm ΔE and 1000-μm E detectors. In this work, only the downstream telescope has been considered; it detected the majority of particle events and was located 1.6 cm from the target, providing an angular coverage of 28° to 56°. Suppression of δ electrons was accomplished with a 12.5-μm-thick Al foil and a 2-mm-thick Al plate spanning the front and back of the particle telescope, respectively.

The energy calibration of individual silicon detectors was obtained from an α-emitting ^{226}Ra source. Germanium detector energy and efficiency calibrations were performed using a ^{152}Eu γ-ray source at low γ-ray energies, and the ^{12}C$(d,p\gamma)\,^{13}$C and ^{13}C$(d,p\gamma)\,^{14}$C reactions for higher energies. The γ-ray photopeak detection efficiencies in add-back mode were 1.0(1)%, 0.53(6)%, and 0.26(3)% at 1 MeV, 3.09 MeV, and 6.90 MeV, respectively.

Several independent hardware triggers were recorded: (i) particle-γ, (ii) γ-γ, and (iii) particle single events. Particle-γ coincidences of γ-ray multiplicity 1 or greater were recorded if they were associated with a particle detected in the ΔE-E telescope within a 550 ns coincidence window. However, only the proton channel was considered in the present analysis.

III. DATA ANALYSIS

The data were analyzed offline, with a reduced coincidence window of 100 ns between γ and p events, using the TSCAN [22] and GNUSCOPE [23] packages. The detected proton energies were corrected for recoil effects and energy losses through the target and Al δ-electron shields. From well-resolved low-lying levels populated directly in the reaction, the energy resolutions (full width at half maximum, FWHM) of the ΔE-E telescope was measured to be ∼200 keV.

The target contained some ^{12}C and ^{16}O contamination. As the γ decays of the corresponding reaction products (^{13}C and ^{17}O) are well known, the transitions from these isotopes were removed from consideration.

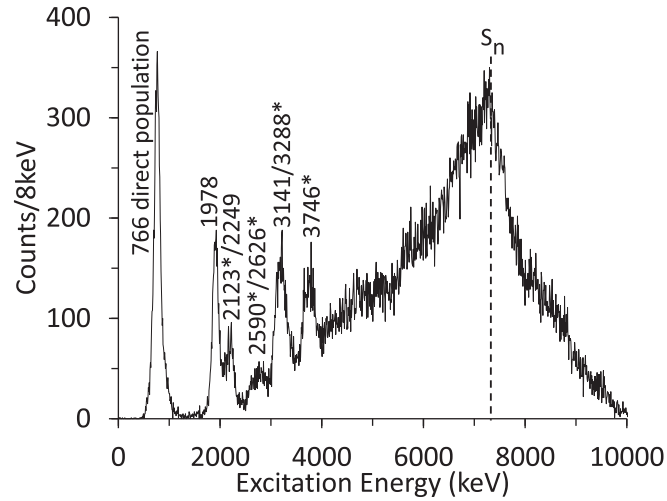

FIG. 1. Proton-energy spectrum gated by the 766 keV $7/2^+_1 \rightarrow 5/2^+_1$ transition in ^{95}Mo. The horizontal axis shows the excitation energy which corresponds to the detected proton energy. The peak at the lowest excitation energy (highest proton energy) is the direct population of the 766-keV level. Strong peaks are labeled by their excitation energies and states observed for the first time are marked with asterisks. The location of the neutron separation energy is indicated by the vertical dashed line.

A. Construction of level scheme

The ^{95}Mo level scheme was constructed using different coincidence spectra:

(1) We exploited proton-energy spectra in coincidence with a well-known γ transition deexciting a discrete level. This type of spectrum allows for a clear identification of the excitation energy, directly populated in the (d,p) reaction, and subsequently decays (directly or via a γ-ray cascade) to a lower-lying level. An example of such a spectrum, gated on the $E_\gamma = 766$ keV transition deexciting the $J^\pi = 7/2^+$ 766-keV level, is shown in Fig. 1.

(2) We utilized γ-ray spectra from different excitation energies of the nucleus which are defined by the detected proton energies. Figure 2 shows three examples of such γ-ray spectra, gated by 200-keV wide excitation energy slices. This illustrates the dependence of the observed γ-ray spectra on initial excitation energy E_i, and allows for a unique identification of transitions to the ground state ($E_i = E_\gamma$), among others.

(3) From p-γ-γ coincidences, γ-ray spectra gated on well-resolved transitions decaying to discrete levels were constructed. No specific proton energy was required for the construction of these spectra. Examples of such spectra, in coincidence with the 204-keV transition from the $J^\pi = 3/2^+$ 204-keV level and the 1073-keV transition from the $J^\pi = 7/2^+$ 1073 keV-level, are shown in Fig. 3.

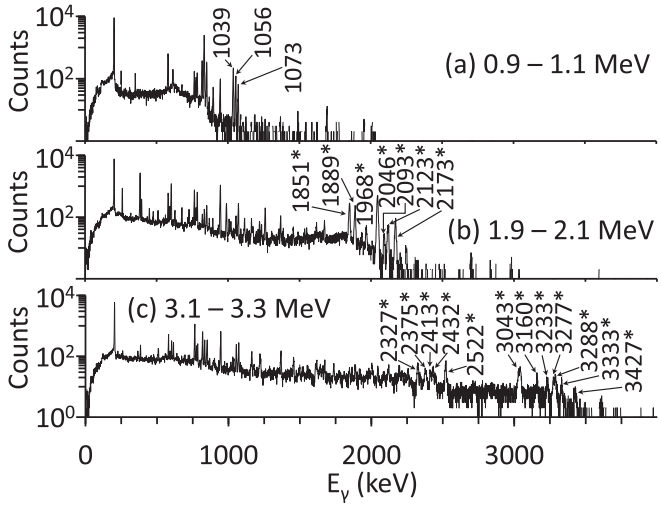

FIG. 2. Spectra of γ rays from different initial excitation energies: (a) 0.9–1.1 MeV, (b) 1.9–2.1 MeV, and (c) 3.1–3.3 MeV. Initial excitations are defined by the detected proton energy with a resolution of ~200 keV FWHM. The strongest high-energy transitions are labeled by their energies. Previously unknown transitions are marked by asterisks.

B. Spin determination of levels

1. Traditional methods

Information on the spins of levels is traditionally obtained using two different methods: (1) measurement of angular distributions in transfer reactions, and (2) applying restrictions on spins from the low-lying γ-decay scheme using selection rules for γ and β decay. It has also been shown that spins of well-populated higher-lying levels, where the level density is typically large, can be successfully extracted from particle and γ-ray gated angular distribution measurements [24]. In the case of ^{95}Mo, the spins of many low-lying levels have been determined extensively and repeatedly in many excellent measurements [25]. None of the above mentioned methods will add significantly improved or new information from our data.

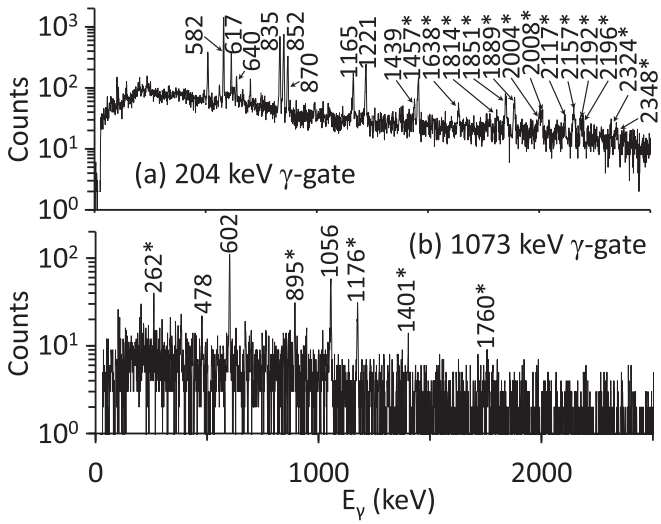

FIG. 3. Spectra of γ rays in coincidence with a proton of arbitrary energy and (a) the 204 keV $3/2_1^+ \rightarrow 5/2_1^+$ and (b) 1073 keV $7/2_2^+ \rightarrow 5/2_1^+$ transitions. Transitions unambiguously assigned to the level scheme of ^{95}Mo are labeled by their energies. Previously unknown transitions are marked by asterisks. The presence of the transition at 1056 keV in panel (b) is indicative of the 1073 keV doublet nature and that it originates from levels at 1073 and 2129 keV (see level scheme for details).

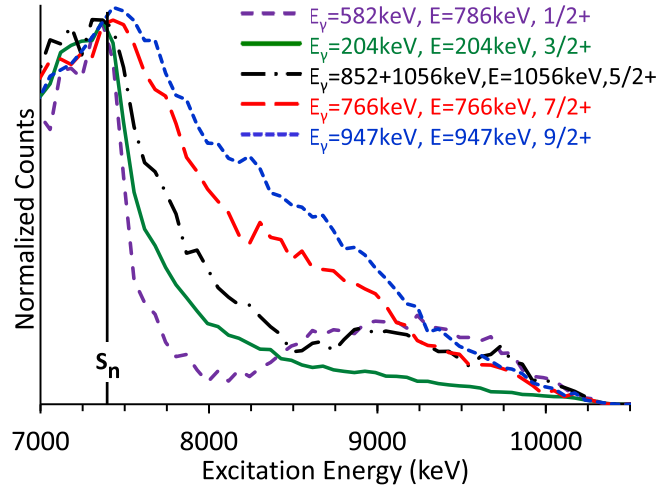

FIG. 4. Proton-energy spectra, in the vicinity of the neutron separation energy, gated on low-lying discrete transitions. The horizontal axis shows the excitation energy in ^{95}Mo deduced from detected proton energies. The increase in the proton signals, peaking at $\approx$ 9 MeV for the 852+1056 and 582 keV gated spectra, is due to contributions from (n,n') reactions on the ^{72}Ge and ^{76}Ge isotopes in the clover crystals, respectively (see text for details). The vertical line indicates the location of the neutron separation energy, and the signals were summed into 62 keV/channel bins.

2. Novel method

The spectra of proton energies, gated on a specific γ-ray from low-lying levels, are suitable not only for gaining information regarding the energies of levels and their decay pattern, but also for the determination of the spins of these levels. This determination can be accomplished by examining the behavior of the energy dependence of the proton spectra just above S_n, as shown in Fig. 4. The different spectra in this figure were normalized just below S_n. Evidently, the energy dependence of the number of counts in the proton spectra above S_n depends on the spins of low-lying levels. This effect has been observed previously [5,9] and was interpreted as the influence of the centrifugal barrier on the emission of neutrons from unbound states [4]. However, its application to assigning spin to a low-lying level has, according to our knowledge, never been discussed.

In Fig. 4, a bump near 9 MeV is visible in gates on the 582- and 852-keV transitions. This characteristic feature is due to neutrons released from states in ^{95}Mo above S_n, populated in the (d,p) reaction. Some of these neutrons undergo (n,n') scattering in the Ge crystals of the γ-ray detectors. The effect

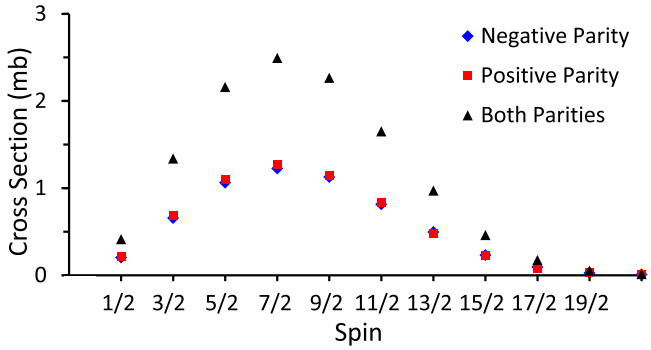

FIG. 5. Spin distribution for the ^{94}Mo(d,p) reaction at 11 MeV beam energy, populating states between 7.15 to 7.51 MeV excitation energies in ^{95}Mo, as calculated with TALYS [27].

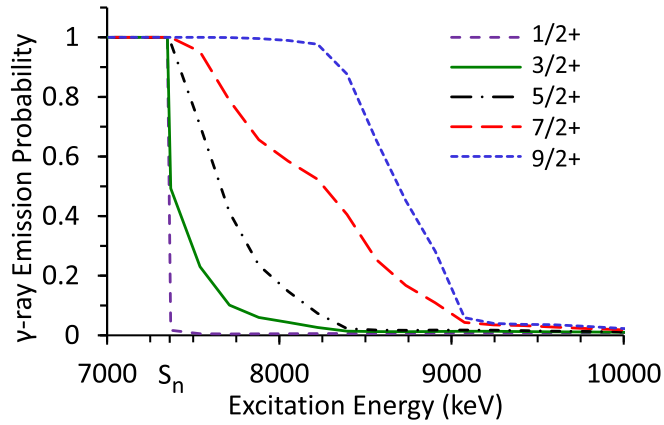

FIG. 6. Predictions of average γ-ray emission probabilities from TALYS [27] for five different initial spins in the vicinity of S_n for ^{95}Mo. Levels of both parities are included for each J. The results are displayed in 170-keV-wide bins.

on γ rays emitted from the recoiling Ge isotopes manifests itself as a high-energy tail of ∼100 keV in the γ-ray spectra [26]. As such, gated γ-ray transitions (582 and 852 keV in our case) that lie on the recoil tails (from 834 and 563 keV $2_1^+ \rightarrow 0_1^+$ transitions in ^{72}Ge and ^{76}Ge, respectively) will contain contributions from these n-p-γ coincidence events.

The different shapes of the proton spectra above S_n in Fig. 4 are due to (i) different ratios of γ and neutron emission probabilities from levels with different spins produced above S_n, (ii) high level density in the region around S_n, and (iii) low γ-ray multiplicity for feeding low-lying levels, which is responsible for the different distributions of spins for levels above S_n that participate in feeding the low-lying levels. These conditions are combined with the fact that the initial distribution of spins of levels populated in the (d,p) reaction is rather broad. This is illustrated in Fig. 5, where predictions of the spin distribution of populated levels in this reaction near S_n is obtained from TALYS simulations [27] utilizing the level density model from Ref. [28]. Both positive- and negative-parity states are expected to be populated with very similar cross sections. This predicted spin distribution is similar for all excitation energies and is reasonably consistent with experimental data, where we observe that levels up to $J = 11/2$ are strongly populated in the (d,p) reaction (we also observe a weak population of a $J = 13/2$ 2058 keV level). The highest spin states, observed in our data, are the $J = 15/2$ and $J = 17/2$ levels at $E_x = 2232$ keV and 2580 keV, respectively, but these are entirely due to indirect feeding from higher-lying states and no direct population contribution could be identified.

Levels with energies up to several MeV above S_n can decay only by the emission of photons (described by the probability Γ_γ) or neutrons (described by the probability Γ_n), since charged-particle emission is negligible at these energies. The different Γ_γ or Γ_n emissions for levels with different spins are a consequence of the relatively high energies of the lowest-excited states in ^{94}Mo: 871 and 1574 keV for the 2_1^+ and 4_1^+ states, respectively. This implies that the probability for emission of a neutron from ^{95}Mo significantly decreases with spin of the level just above S_n, as it is not easy to emit neutrons with high angular momenta [4,29] to populate the low-lying, low-spin states in ^{94}Mo. The expected probability of Γ_γ with respect to $\Gamma_n + \Gamma_\gamma$ was calculated with the TALYS reaction code and is shown in Fig. 6. Higher-spin states retain neutrons more efficiently beyond S_n as compared to states of lower spins. It should be noted that the TALYS calculations give the probability integrated over all solid angles and include both parities for each value of J.

The decay paths of levels directly populated in the (d,p) reaction above S_n to specific low-lying levels might be complicated. However, our experimental data (Fig. 4) indicate that an overall "memory" of initial spin is retained, which is in agreement with the expectation that the average multiplicity to reach a low-lying level is relatively small [30,31]. The feeding of low-lying levels has been investigated by performing statistical simulations with the Monte Carlo γ-ray cascade simulation code DICEBOX [32]. The parameters of the photon strength function and nuclear level density in these calculations correspond to the best choice parameters from the analysis of (n,γ) data in ^{96}Mo [30,33] and ^{98}Mo [34]. Instead of calculating the average multiplicity of the cascades, we investigate the fraction F of events from initial states i, with spin and parity J_i^π near S_n which feeds a selected low-lying level. The advantage of this quantity lies in its complete independence of the experimentally unknown cross sections of levels with J_i^π in the (d,p) reaction.

The absolute values of F can be expected to substantially decrease with the excitation energy of a low-lying level. In thermal neutron capture [35] and (γ,γ') experiments [36], the feeding of low-lying levels with the same spin and parity decreases exponentially with their excitation energy. This exponential dependence is also predicted in the DICEBOX simulations of our experiment, although it is not shown here explicitly. However, we are not interested in the absolute values of F, but the dependence of F on the J_i^π of levels populated in the (d,p) reaction above S_n. The spin dependence from DICEBOX simulations is visualized for several low-lying levels in Fig. 7. For the purpose of this comparison, the value of F for each level has been renormalized to allow for a qualitative comparison of the evolution of F with J_i^π.

From Fig. 7(a), it is apparent that the predicted dependence of F on J_i^π differs rather significantly for low-lying levels

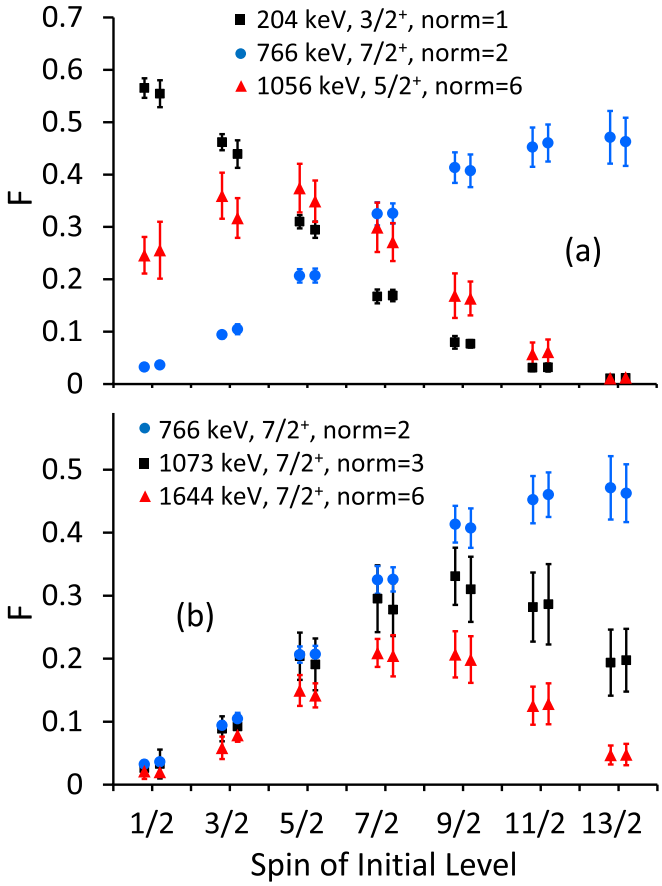

FIG. 7. Simulated dependence of the fraction of events, F, from initial states to selected low-lying levels, as a function of spin of initial levels J_i. A 100-keV wide interval around 7.7-MeV excitation energy was used for the initial levels. The values of F for (a) different low-lying spin levels and (b) low-lying levels of the same spin have been normalized for the purpose of a better comparison. The normalization factors (norm) are given in the legends. Each pair of points near an initial spin corresponds to positive and negative-parity levels with J_i. Uncertainties are due to different nuclear realizations of the level scheme [32].

with different spins; this is consistent with our experimental data. As could be expected, the low-lying levels with higher spins have a substantially higher feeding from states of higher J_i^π, populated in the (d,p) reaction above S_n. At the same time, Fig. 7(b) indicates that the distribution of F is similar (but not identical) for all low-lying levels with the same spin. Here, the more "localized" distribution of F with increasing excitation energy of a low-lying level comes from the fact that levels with very low excitation energy can collect transitions from a broader distribution of initial spins J_i. However, the predicted difference in the distribution of F for low-lying levels with the same spin is in all cases significantly smaller than the difference in distributions of low-lying levels with different spins. Furthermore, simulations indicate virtually no dependence of F for a fixed low-lying level on initial excitation energy between 7.3 and 9 MeV. These calculations support our approach to utilize the region around S_n to determine the spin of low-lying levels in ^{95}Mo.

The shape of the γ-ray gated proton-energy spectra just above S_n, shown in Fig. 4, is given by a folding of (i) distribution of initial spins from the (d,p) reaction (Fig. 5), (ii) the emission probability for γ transitions (Fig. 6), (iii) the fraction F feeding corresponding low-lying levels (Fig. 7), and (iv) the experimental proton energy detection resolution.

The determination of spins of low-lying levels from the shape of proton spectra above S_n is complementary to the methods mentioned in Sec. III B 1. Since the present method involves an integral of counts over all detection angles, it may be used even if the population of a state is weak or the angular distribution cannot be measured for other reasons. The proposed method can be used to determine the spins of levels in many nuclei prepared in any direct reaction [i.e., not only through the (d,p) reaction], which populates a broad range of spins above S_n, as long as the coincidence between the outgoing charged particle and a γ-ray line deexciting the level of interest is measured. The only strong restrictions on the applicability of the novel method are the following:

(1) The particle energy resolution has to be better than the energy differences between low-lying levels in the residual nuclei which are populated following neutron emission. The presence of a suitable nuclear structure of low-lying levels in the residual nuclei is necessary. Good candidates for determining spins are even-Z, odd-N nuclei, for which the even-even nuclei (i.e., after neutron emission) have 2_1^+ and 4_1^+ excitation energies of at least several hundred keV.

(2) In order to obtain the characteristic spin-dependent feature in the vicinity of S_n, the level density has to be high enough to result in a smooth spin-dependent distribution. For nuclei with large proton-to-neutron asymmetries and for systems with few active nucleons where the level density is small, fluctuations of neutron widths in combination with the distribution of reaction cross sections may be problematic. In this regime, our method of spin determination may not be applicable and other approaches will have to be considered.

IV. RESULTS AND DISCUSSION

A. Levels and γ-ray transitions

The use of high-resolution γ-ray detectors allows for a significant improvement in resolving and determining level energies, particularly at high-excitation energies. The comparison of the observed levels to those from previous works is challenging above an excitation energy of $\approx$3 MeV, due to the high level density and general large experimental uncertainties of earlier measurements. Our identification of levels is mainly based on previous (d,p) reaction studies. Matches were not attempted for states populated and reported from other reactions above $\approx$3 MeV. Whenever γ-ray transitions were reported previously, these were also utilized to identify and match levels. All reported branching ratios were determined from our data. The level scheme is summarized in Table I, and includes all levels and transitions observed in this work. Comparisons to previous results as compiled in the Evaluated Nuclear Structure Data File (ENSDF) [25] are made where

TABLE I. Comparison of the level scheme from the ENSDF [25] with our (d,p) experiment. Excitation energies of levels E, level spins and parities J^π, energies of γ rays deexciting a level E_γ, as well as the final level E_f are provided. Spins from our measurement (column 5) are exclusively obtained from the novel method described in Sec. III B 2. The measured branching ratios, BR, are normalized to the strongest transition originating from each level. The spin and parity of the final level, J_f^π, (last column) is inferred from a combination of our results and ENSDF assignments. All previously reported levels and γ-ray transitions are included, as long as these were observed in this work and could be matched to previous measurements. Blank entries indicate the absence of data.

E (keV) [25]	J^π [25]	E_γ (keV) [25]	E (keV) (d,p)	J (d,p)	E_γ (keV) (d,p)	BR (%) (d,p)	E_f (keV) (d,p)	J_f^π [25] + (d,p)
204.1163(16)	$3/2^+$	204.1161(17)	204	3/2	204	100	0	$5/2^+$
765.803(8)	$7/2^+$	765.791(9)	766	7/2	766	100	0	$5/2^+$
786.201(3)	$1/2^+$	786.198(4)	786	1/2	786	30(5)	0	$5/2^+$
		582.08293)			582	100	204	$3/2^+$
820.628(4)	$3/2^+$	820.624(5)	820	3/2	820	100	0	$5/2^+$
		616.49(3)			617	27(4)	204	$3/2^+$
947.685(16)	$9/2^+$	947.677(19)	947	9/2	947	100	0	$5/2^+$
1039.269(4)	$1/2^+$	1039.264(7)	1039	1/2	1039	11(2)	0	$5/2^+$
		835.149(5)			835	100	204	$3/2^+$
		253.067(9)			253	3(1)	786	$1/2^+$
		218.640(8)			219	<1	820	$3/2^+$
1056.771(20)	$5/2^+$	1056.798(25)	1056[a]	5/2	1056	43(7)	0	$5/2^+$
		852.61(4)			852	100	204	$3/2^+$
1073.727(16)	$7/2^+$	1073.72(4)	1073[a]	7/2	1073	100	0	$5/2^+$
		869.60(3)			870	17(10)	204	$3/2^+$
1369.75(12)	(3/2)	1369.76(13)	1369	3/2	1369	100	0	$5/2^+$
		1165.5(3)			1165	48(8)	204	$3/2^+$
1425.992(24)	$(5/2)^+$ [a]	1426.11(15)	1426	3/2[a]	1426	2(1)	0	$5/2^+$
		1222.00(3)			1221	100	204	$3/2^+$
		640.0(3)			640	30(5)	786	$1/2^+$
1540.801(13)	$11/2^+$	774.989(11)	1541	11/2	775	66(13)	766	$7/2^+$
		593.15(5)			593	100	947	$9/2^+$
1551.772(18)	$(9/2)^+$	1551.71(5)	1551		1551	5(2)	0	$5/2^+$
		785.929(20)			786	48(8)	766	$7/2^+$
		604.02(6)			604	100	947	$9/2^+$
		(495.19)			495	<1	1056	$5/2^+$
		477.7(4)			478	6(2)	1073	$7/2^+$
1620.26(3)	$3/2^+$	1620.20(4)	1619	3/2	1619	100	0	$5/2^+$
		1416.09(8)			1415	5(2)	204	$3/2^+$
		799.60(15)			799	4(1)	820	$3/2^+$
		563.48(6)			563	19(3)	1056	$5/2^+$
(1645.1(6))	$7/2^{(+)}$	(1645.0(9))	1644	7/2	1644	87(14)	0	$5/2^+$
		(1441.0(9))			1439	100	204	$3/2^+$
(1660.3(3))	$(\leqslant 5/2)^a$		1661	$3/2^a$	1457[a]	100	204	$3/2^+$
1667(8)	$7/2^+, 9/2^+$ [a]		1676	$9/2^a$	1676	85(19)	0	$5/2^+$
					728	100	947	$9/2^+$
					602	82(17)	1073	$7/2^+$
			1842	7/2	1638	54(11)	204	$3/2^+$
					1021	100	820	$3/2^+$
1888.54(22)[a]	$(9/2)^+$ [a]		1880[a]	$9/2^a$	933	100	947	$9/2^+$
		(337.3(3))[a]			338[a]	20(4)	1541	$11/2^+$
1937.47(7)	$11/2^-$	990.4(3)	1937	11/2	990	23(4)	947	$9/2^+$
		396.46(17)			396	13(2)	1541	$11/2^+$
		(385.82(9))			386	100	1551	$(9/2)^+$
					262	28(5)	1676	$9/2^+$
1963[a]	$3/2^+, 5/2^+$ [a]		1968[a]	$5/2^a$	895	100	1073	$7/2^+$
1984(15)[a]	$3/2^+, 5/2^+$ [a]		1978[a]		1212	13(3)	766	$7/2^+$
					1032	100	947	9/2
2045(3)	$(3/2)^+$		2046		2046	100	0	$5/2^+$
					1261	16(3)	786	$1/2^+$
2049	$1/2^+$		2055	1/2	1851	100	204	$3/2^+$
2058.51(7)	$(13/2^+)$	1110.75(10)	2058	$\geqslant 13/2$	1111	100	947	$9/2^+$

TABLE I. (*Continued.*)

E (keV) [25]	J^π [25]	E_γ (keV) [25]	E (keV) (d,p)	J (d,p)	E_γ (keV) (d,p)	BR (%) (d,p)	E_f (keV) (d,p)	J_f^π [25] + (d,p)
2089	$(3/2)^+$		2093		2093	16(3)	0	$5/2^+$
					1889	100	204	$3/2^+$
2118	$7/2^+, 9/2^+$		2123		2123	100	0	$5/2^+$
					1357	19(4)	766	$7/2^+$
			2129		1073	100	1056	$5/2^+$
2169(15)	$(3/2)^+$		2173		2173	100	0	$5/2^+$
					1968	21(4)	204	$3/2^+$
					1387	16(3)	786	$1/2^+$
					1116	25(4)	1056	$5/2^+$
2213(4)	$1/2^-, 3/2^-$		2212		2008	100	204	$3/2^+$
2232.27(7)	$(15/2)^+$	691.45(9)	2232	$\geqslant 13/2$	691	100	1541	$11/2^+$
2244	$(3/2)^+$		2249		2249	100	0	$5/2^+$
					1484	32(6)	766	$7/2^+$
					1192	18(3)	1056	$5/2^+$
					1176	74(12)	1073	$7/2^+$
			2285		1499	100	786	$1/2^+$
			2291		1525	16(4)	766	$7/2^+$
					1344	100	947	$9/2^+$
2315(8)	$1/2^-, 3/2^-$		2321		2117	100	204	$3/2^+$
			2349		1402	100	947	$9/2^+$
2357	$1/2^+$		2361		2361	9(2)	0	$5/2^+$
					2157	100	204	$3/2^+$
2383[a]	$(3/2)^+$ [a]		2386[a]		2386	100	0	$5/2^+$
					1438[a]	16(3)	947	$9/2^+$
2396(10)	$(3/2)^+$		2396		2192	100	204	$3/2^+$
			2400		2196	100	204	$3/2^+$
					1032	82(14)	1369	(3/2)
2428(13)	$7/2^+, 9/2^+$		2432		1485	100	947	$9/2^+$
			2474		1401	100	1073	$7/2^+$
			2483	9/2	424	100	2058	$(13/2^{(+)})$
			2511		1564	100	947	$9/2^+$
			2528[a]		2324	100	204	$3/2^+$
					1581	21(4)	947	$9/2^+$
2544	$(1/2^-, 3/2^-)$		2552		2348	100	204	$3/2^+$
2580.08(10)	$(17/2)^+$	347.89(9)	2580	$\geqslant 13/2$	348	100	2232	$(15/2)^+$
			2590		1824	100	766	$7/2^+$
2595	$1/2^+$		2600		1814	100	786	$1/2^+$
					1561	43(7)	1039	$1/2^+$
					981	20(4)	1619	$3/2^+$
2611.14(12)	$(15/2^-)$	673.88(20)	2611	$\geqslant 13/2$	674	100	1937	$11/2^-$
		552.45(16)			552	23(5)	2058	$(13/2^{(+)})$
			2626		1860	100	766	$7/2^+$
2695	$(3/2^+)$		2697		2697	100	0	$5/2^+$
2745	$(3/2^+)$		2751		2547	100	204	$3/2^+$
					1931	63(11)	820	$3/2^+$
2754	$3/2^+$		2759		2759	100	0	$5/2^+$
2830	$(3/2)^+$		2816		2050	100	766	$7/2^+$
2843	$(3/2)^+$		2834		2834	91(16)	0	$5/2^+$
					1888	100	947	$9/2^+$
					1760	94(16)	1073	$7/2^+$
			2961		2014	100	947	$9/2^+$
3037	$3/2^+$		3043		3043	100	0	$5/2^+$
					2257	30(5)	786	$1/2^+$
					2004	42(7)	1039	$1/2^+$
					1987	24(3)	1056	$5/2^+$
					1674	16(3)	1369	(3/2)

TABLE I. (*Continued.*)

E (keV) [25]	J^π [25]	E_γ (keV) [25]	E (keV) (d,p)	J (d,p)	E_γ (keV) (d,p)	BR (%) (d,p)	E_f (keV) (d,p)	J_f^π [25] + (d,p)
3142	$(3/2)^+$		3141		2375	100	766	$7/2^+$
			3147		2380	59(10)	766	$7/2^+$
					2327	100	820	$3/2^+$
3155	$3/2^+, 5/2^+$		3160		3160	100	0	$5/2^+$
			3198		2432	100	766	$7/2^+$
			3216		3216	100	0	$5/2^+$
			3233		3233	100	0	$5/2^+$
					2413	99(19)	820	$3/2^+$
			3277		3277	100	0	$5/2^+$
			3288		3288	68(13)	0	$5/2^+$
					2522	100	766	$7/2^+$
			3333		3333	100	0	$5/2^+$
			3427		3427	100	0	$5/2^+$
			3495		3495	100	0	$5/2^+$
			3600		3600	100	0	$5/2^+$
			3746		3746	100	0	$5/2^+$
					2982	51(9)	766	$7/2^+$
			3877		3877	100	0	$5/2^+$
			3944		3944	100	0	$5/2^+$
			3992		3992	100	0	$5/2^+$
			4092		4092	100	0	$5/2^+$
			4140		4140	100	0	$5/2^+$
			4195		4195	100	0	$5/2^+$
			4239		4239	100	0	$5/2^+$
			4329		4329	100	0	$5/2^+$
			4407		4407	100	0	$5/2^+$
			4461		4461	100	0	$5/2^+$
			4565		4565	100	0	$5/2^+$
			4675		4471	100	204	$3/2^+$
			4791		4791	100	0	$5/2^+$
			4847		4847	100	0	$5/2^+$
			5583		5583	100	0	$5/2^+$
			5678		5678	100	0	$5/2^+$
			5889		5889	100	0	$5/2^+$
			5972		5972	100	0	$5/2^+$
			6064		6064	100	0	$5/2^+$

[a]See text for details.

possible. For clarity, important features of low-lying levels that differ from the ENSDF [25] are elaborated on in more detail in the text. The uncertainties in γ-ray energies range from 1 keV for transitions below 1 MeV and gradually increase to 3 keV for the highest observed transition energy at 6064 keV. The uncertainties in excitation energies are expected to be of the same order.

Several transitions with previously uncertain placement within the level scheme, level energies, and spin assignments, were confirmed, removed, or corrected. Almost all spins for levels below excitation energies of 2.1 MeV were determined with the novel method described in Sec. III B 2. Discrete states of high-excitation energies are plentiful. However, the corresponding high-energy γ-ray transitions, which have a larger FWHM, overlap in the spectrum with other transitions, prohibiting a clean spin assignment. Generally, the only spins that could be determined from high-lying levels are those that decay through low-energy transitions.

1. Level: 1056 keV

This level is directly populated in our measurement. It has also been reported in other (d,p) measurements [37,38]. For reasons unknown, this level has not been included in the (d,p) section of the ENSDF [25]. A 237-keV transition, with a large branching ratio of 70% was reported in a fusion-evaporation reaction measurement [39] and tentatively assigned to the 1056-keV level [25]. This γ-ray decay branch could not be confirmed in this work.

2. Level: 1073 keV

Although, the 1073-keV level has never been reported in a (d,p) measurement, a peak is clearly visible in the particle spectra of Ref. [37]. It is also observed to be directly populated in our (d,p) study. A 253-keV γ ray with intensity of 32(32)% has been reported to originate from this 1073-keV level [39], but this transition could not be observed in our measurement.

3. Level: 1426 keV

Although the ENSDF database tentatively assigns $J = 5/2$ to the 1426-keV level [25], it was previously reported as $J^\pi = 3/2^+$ in Refs. [37,40,41]. A $J = 3/2$ spin assignment agrees with the present analysis.

4. Level: 1661 keV

The 1660-keV level and a $E_\gamma = 1660$-keV γ-ray transition were assigned tentatively in Ref. [25]. While the level is observed in our experiment, we cannot identify a 1660-keV transition. However, a transition $E_\gamma = 1457$ keV to the first excited 204-keV level was clearly observed. The energy dependence of the proton spectrum above S_n exhibits $J = 3/2$ characteristics which is consistent with the assignment of $J \leqslant 5/2$ [25].

5. Level: 1676 keV

We clearly observe a level at this energy which we identify with the $J^\pi = 7/2^+,9/2^+$ level at 1667(8) keV [25]. Our spin assignment yields $J = 9/2$ for this level, which is consistent with the observation of a 262-keV transition to the $J = 11/2^-$ 1937 keV level.

6. Level: 1880 keV

A level at 1879(12) keV with $J^\pi = 9/2^+$ was previously reported [40]. The tentative assignment of $J = 9/2$ and its 338-keV transition has been confirmed. In Ref. [25] a 337.3-keV transition was assigned to the level at 1888.5(2) keV. However, based on our observation, which is also corroborated by Ref. [39], the 1888.5-keV level has been either misplaced or mislabeled. The correct level energy is 1880 keV.

7. Level: 1968 keV

We observe a level at 1968 keV with $J = 5/2$, in agreement with previous results from a (d,p) reaction [37]. This level likely corresponds to the previously reported $J = 3/2^+,5/2^+$ level at 1963 keV [25].

8. Level: 1978 keV

We assume that this level is the 1984(15)-keV state with $J^\pi = 3/2^+,5/2^+$ observed using (p,t) and (d,t) reactions [25]. We were unable to determine the spin with our novel method, but the observed γ-ray decay to the $J = 9/2^+$ 947-keV level strongly favors the $J^\pi = 5/2^+$ assignment to the 1978-keV level.

9. Level: 2386 keV

If we assume that this state is equivalent to the 2383-keV level previously observed in several (d,p) reactions [25], then the tentative $J = 3/2$ assignment from Ref. [25] is not consistent with the observed $E_\gamma = 1438$-keV transition to the $J^\pi = 9/2^+$ 947-keV level.

10. Level: 2528 keV

Although we could in principle assume that the observed level is the same as the one reported at 2531(12) keV with $J^\pi = 9/2^+$ [25], the newly observed γ decay to a $3/2^+$ level does not support a $J^\pi = 9/2^+$ assignment. The strong experimental evidence for a $J^\pi = 9/2^+$ assignment to the 2531(12)-keV level from several other measurements [40–42], together with our observation of a γ-ray decay to a $3/2^+$ levels indicates that there is a close doublet structure at this energy. As such, the state at 2528 keV observed here is a new addition to the level scheme.

11. Levels between 3200 and 4860 keV

We observe many levels in this energy range, but we are unable to reliably match these with levels from previous measurements. The majority of the levels previously reported above 3200 keV were observed in (p,t) [40] and (p,d) [41] reactions, albeit with uncertainties up to 30 keV in the level energies. This large energy uncertainty, together with the high-level density in this energy region, makes a definitive comparison between our results and previously observed levels impossible. The analysis is further complicated due to the absence of information on levels populated in previous (d,p) measurements above an excitation energy of 3.16 MeV.

B. Comparison with shell model predictions

We now compare experimental data at low-excitation energies (<2.3 MeV) with predictions from the m-scheme shell model code COSMO [43]. For protons, our model space contains the $2p_{1/2}$ and $1g_{9/2}$ valence orbits which are below the $Z = 50$ magic number. For neutrons the valance space includes $3s_{1/2}$ and $2d_{5/2}$ orbits that are above $N = 50$. The calculations are based on the *gl* interaction [44], and the results are compared to experimental energy levels in Fig. 8.

This simple shell model calculation is intended to only provide a brief overview of the underlying structures of some low-energy gross features. The model correctly predicts the ordering of low-lying levels, beginning with the ground

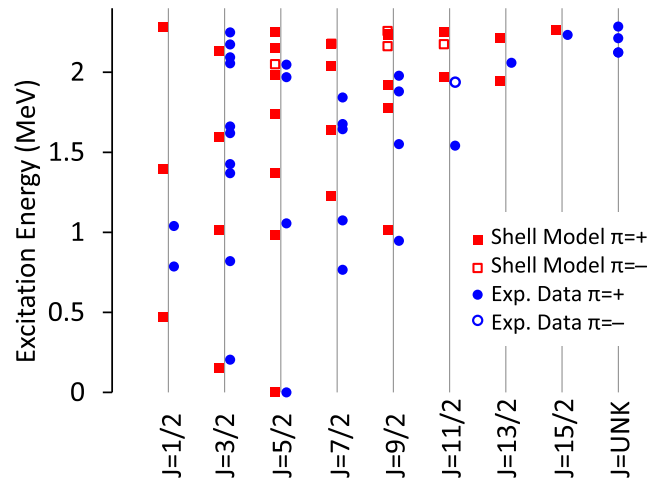

FIG. 8. Comparison of levels in ^{95}Mo predicted by the shell model (squares) and populated in the (d,p) reaction (circles). Positive-parity and negative-parity levels are indicated by filled and open symbols, respectively. The levels are separated into columns depending on their spin value. The last column $J =$ UNK includes experimental levels of unknown spins.

state $J^\pi = 5/2^+$, followed by the first-excited state of $J^\pi = 3/2^+$. Overall, the first level of any spin value is predicted correctly within an energy range of less than ≈300 keV, except for the first $7/2^+$ level and $11/2^+$ where differences between theoretical and experimental values of 463 keV and 431 keV are observed, respectively. The shell model reveals the exclusive population of positive-parity states for energies below 2 MeV.

Predicted negative-parity states start to appear just above 2 MeV. Experimentally, the first negative-parity level is observed at 1937 keV with $J^\pi = 11/2$, and calculated at an energy of 2174 keV. Above excitation energies of ∼2.3 MeV, negative-parity states are being populated approximately as frequently as positive-parity levels, up to the highest calculated energy of 3.5 MeV. The overall good agreement in the low-energy level structure is indicative that the *gl* interaction provides a satisfactory description of the single-particle levels in ^{95}Mo.

The ground state of ^{95}Mo can be described as a $N = 50$ closed shell with the three remaining neutrons in the $2d_{5/2}$ orbit, while the protons are found in the $1g_{9/2}$ orbit; this explains the good agreement with the shell model results. As discussed in Ref. [45], levels with $J \geqslant 13/2$ are predominantly due to the alignment of mixed proton-neutron configurations. As such, the low-lying excited states are due to neutron configurations with wave function components predominantly from the $2d_{5/2}$, $1g_{7/2}$, $3s_{1/2}$, and $2d_{3/2}$ orbits. To some extent this is confirmed by our limited shell model study. The emergence of the experimentally observed first negative-parity state $J^\pi = 11/2^-$ has been linked to the $1h_{11/2}$ intruder configuration [46]. A lowering of level energy due to the admixture of intruder configurations explains why the shell model predicts this and some other states to be higher in energy. Configurations specific to the low-lying levels and particle occupations of the various single-particle levels have been discussed in detail [37–42,45,46].

V. SUMMARY

Levels in ^{95}Mo were populated in the (d, p) reaction at a beam energy of 11 MeV. Protons and γ radiation were detected with silicon particle telescopes and an array of Clover detectors, respectively. The γ-decay properties of ^{95}Mo were investigated using p-γ(-γ) coincidence information. The level scheme was significantly expanded for excitation energies up to about 6 MeV, and 102 new transitions and 43 new states were observed. The low-lying levels are reasonably well described with shell model calculations using the *gl* interaction.

The spacing of the lowest excited states in ^{94}Mo leads to a significant suppression of neutron emission from high-spin levels populated just above S_n in ^{95}Mo. This effect is responsible for a strong spin dependence in the population of low-lying levels in ^{95}Mo. Using data from p-γ coincidences, we utilized these differences to propose a new method for spin determination. We were able to determine spins of almost all ^{95}Mo levels below 2 MeV, and for a few levels above this excitation energy. This technique is complementary to other spin-determining methods and could be used for many nuclei produced in a variety of direct reactions, as long as the coincidence between the outgoing charged particle and a γ ray deexciting the level of interest is measured.

ACKNOWLEDGMENTS

The authors thank the operations staff at the 88-Inch Cyclotron of Lawrence Berkeley National Laboratory for a smooth run. This work is supported by the National Research Foundation of South Africa under Grants No. 92789 and No. 83867. This work is also performed under the auspices of the University of California Office of the President Laboratory Fees Research Program under Award No. 12-LR-238745, the U.S. Department of Energy Lawrence Livermore National Laboratory under contract DE-AC52-07NA27344, Florida State University under DE-SC0009883, and University of Richmond under DE-FG52-06NA26206 and DE-FG02-05ER41379. For Lawrence Berkeley National Laboratory this work was supported by the Director, Office of Science, Office of Nuclear Physics, of the U.S. Department of Energy under Contract No. DE-AC02-05CH11231. M.K. acknowledges support from Grant No. 13-07117S of the Czech Science Foundation. A.C.L. acknowledges support from the ERC-STG-2014 under Grant Agreement No. 637686.

[1] C. Sneden, J. J. Cowan, and R. Gallino, Annu. Rev. Astron. Astrophys. **46**, 241 (2008).
[2] Report of the Nuclear Physics and Related Computational Science R&D for Advanced Fuel Cycles Workshop, DOE Offices of Nuclear Physics and Advanced Scientific Computing Research, August 2006 (unpublished).
[3] W. H. Hannum, G. E. Marsh, and G. S. Stanford, Sci. Am. **293**, 84 (2005).
[4] James Robb Grover, Phys. Rev. **123**, 267 (1961).
[5] G. Stengl *et al.*, Nucl. Phys. A **290**, 109 (1977).
[6] D. R. Slaughter *et al.*, Phys. Lett. B **38**, 22 (1972).
[7] F. M. Nuh *et al.*, Phys. Lett. B **53**, 435 (1975).
[8] C. J. Bischof and W. L. Talbert, Phys. Rev. C **15**, 1047 (1977).
[9] N. D. Scielzo, J. E. Escher, J. M. Allmond, M. S. Basunia, C. W. Beausang, L. A. Bernstein, D. L. Bleuel, J. T. Burke, R. M. Clark, F. S. Dietrich, P. Fallon, J. Gibelin, B. L. Goldblum, S. R. Lesher, M. A. McMahan, E. B. Norman, L. Phair, E. Rodriquez-Vieitez, S. A. Sheets, I. J. Thompson, and M. Wiedeking, Phys. Rev. C **81**, 034608 (2010).
[10] G. Boutoux *et al.*, Phys. Lett. B **712**, 319 (2012).
[11] N. D. Scielzo *et al.*, Phys. Rev. C **85**, 054619 (2012).
[12] A. Ratkiewicz *et al.*, Eur. Phys. J. Web Conf. **93**, 02012 (2015).
[13] S. V. Ilyushkin, J. A. Winger, C. J. Gross, K. P. Rykaczewski, J. C. Batchelder, L. Cartegni, I. G. Darby, C. Goodin, R. Grzywacz, J. H. Hamilton, A. Korgul, W. Królas, S. N. Liddick, C. Mazzocchi, S. Padgett, A. Piechaczek, M. M. Rajabali, D. Shapira, and E. F. Zganjar, Phys. Rev. C **80**, 054304 (2009).

[14] S. V. Ilyushkin, J. A. Winger, K. P. Rykaczewski, C. J. Gross, J. C. Batchelder, L. Cartegni, I. G. Darby, R. Grzywacz, J. H. Hamilton, A. Korgul, W. Królas, S. N. Liddick, C. Mazzocchi, T. Mendez, S. Padgett, M. M. Rajabali, D. Shapira, D. W. Stracener, and E. F. Zganjar, Phys. Rev. C **83**, 014322 (2011).
[15] J. L. Tain, E. Valencia, A. Algora, J. Agramunt, B. Rubio, S. Rice, W. Gelletly, P. Regan, A. A. Zakari-Issoufou, M. Fallot, A. Porta, J. Rissanen, T. Eronen, J. Äystö, L. Batist, M. Bowry, V. M. Bui, R. Caballero-Folch, D. Cano-Ott, V. V. Elomaa, E. Estevez, G. F. Farrelly, A. R. Garcia, B. Gomez-Hornillos, V. Gorlychev, J. Hakala, M. D. Jordan, A. Jokinen, V. S. Kolhinen, F. G. Kondev, T. Martínez, E. Mendoza, I. Moore, H. Penttilä, Z. Podolyák, M. Reponen, V. Sonnenschein, and A. A. Sonzogni, Phys. Rev. Lett. **115**, 062502 (2015).
[16] M. Wiedeking, L. A. Bernstein, M. Krtička, D. L. Bleuel, J. M. Allmond, M. S. Basunia, J. T. Burke, P. Fallon, R. B. Firestone, B. L. Goldblum, R. Hatarik, P. T. Lake, I.-Y. Lee, S. R. Lesher, S. Paschalis, M. Petri, L. Phair, and N. D. Scielzo, Phys. Rev. Lett. **108**, 162503 (2012).
[17] B. L. Goldblum, M. Wiedeking, T. Reed, K. Alfonso, J. M. Allmond, L. A. Bernstein, D. L. Bleuel, F. S. Dietrich, R. Hatarik, P. T. Lake, I.-Y. Lee, S. R. Lesher, S. Paschalis, M. Petri, L. Phair, N. D. Scielzo, R. Vial, and J. Vujic, Phys. Rev. C **85**, 054616 (2012).
[18] S. R. Lesher *et al.*, Nucl. Instrum. Methods Phys. Res., Sect. A **621**, 286 (2010).
[19] G. Duchêne *et al.*, Nucl. Instrum. Methods Phys. Res., Sect. A **432**, 90 (1999).
[20] Z. Elekes *et al.*, Nucl. Instrum. Methods Phys. Res., Sect. A **503**, 580 (2003).
[21] http://www.micronsemiconductor.co.uk.
[22] H.-Q. Jin, TSCAN and related programs: A package to perform tape scanning and to manipulate matrices, Report No. RUTGERS-ORNL-UTK, 1992–1997 (unpublished).
[23] J. Pavan, Ph.D. dissertation, Florida State University, 2004 (unpublished).
[24] J. M. Allmond, C. W. Beausang, J. O. Rasmussen, T. J. Ross, M. S. Basunia, L. A. Bernstein, D. L. Bleuel, W. Brooks, N. Brown, J. T. Burke, B. K. Darakchieva, K. R. Dudziak, K. E. Evans, P. Fallon, H. B. Jeppesen, J. D. LeBlanc, S. R. Lesher, M. A. McMahan, D. A. Meyer, L. Phair, N. D. Scielzo, S. R. Stroberg, and M. Wiedeking, Phys. Rev. C **81**, 064316 (2010).
[25] S. K. Basu *et al.*, Nucl. Data Sheets **111**, 2555 (2010).
[26] I. Abt *et al.*, Eur. Phys. J. A **36**, 139 (2008).
[27] A. J. Koning *et al.*, in *Nuclear Data for Science and Technology*, edited by O. Bersillon *et al.* (EDP Sciences, London, 2008), p. 211; see also http://www.talys.eu.
[28] A. S. Iljinov *et al.*, Nucl. Phys. A **543**, 517 (1992).
[29] *Nuclear Spectroscopy, Part A*, edited by F. Ajzenberg-Selove (Academic Press, New York, 1960).
[30] S. A. Sheets, U. Agvaanluvsan, J. A. Becker, F. Bečvář, T. A. Bredeweg, R. C. Haight, M. Jandel, M. Krtička, G. E. Mitchell, J. M. O'Donnell, W. Parker, R. Reifarth, R. S. Rundberg, E. I. Sharapov, J. L. Ullmann, D. J. Vieira, J. B. Wilhelmy, J. M. Wouters, and C. Y. Wu, Phys. Rev. C **79**, 024301 (2009).
[31] R. Chankova, A. Schiller, U. Agvaanluvsan, E. Algin, L. A. Bernstein, M. Guttormsen, F. Ingebretsen, T. Lönnroth, S. Messelt, G. E. Mitchell, J. Rekstad, S. Siem, A. C. Larsen, A. Voinov, and S. Ødegård, Phys. Rev. C **73**, 034311 (2006).
[32] F. Bečvář, Nucl. Instrum. Methods Phys. Res., Sect. A **417**, 434 (1998).
[33] M. Krtička, F. Bečvář, I. Tomandl, G. Rusev, U. Agvaanluvsan, and G. E. Mitchell, Phys. Rev. C **77**, 054319 (2008).
[34] C. L. Walker *et al.*, Phys. Rev. C **92**, 014324 (2015).
[35] M. Krtička, R. B. Firestone, D. P. McNabb, B. Sleaford, U. Agvaanluvsan, T. Belgya, and Z. S. Revay, Phys. Rev. C **77**, 054615 (2008).
[36] J. Isaak *et al.*, Phys. Lett. B **727**, 361 (2013).
[37] J. B. Moorhead and R. A. Moyer, Phys. Rev. **184**, 1205 (1969).
[38] Sven A. Hjorth and Bernard L. Cohen, Phys. Rev. **135**, B920 (1964).
[39] L. Mesko *et al.*, Nucl. Phys. A **181**, 566 (1972).
[40] P. K. Bindal *et al.*, Phys. Rev. C **15**, 2006 (1977).
[41] S. A. Sultana, D. Maki, G. Wakabayashi, Y. Uozumi, N. Ikeda, F. Syafarudin Aramaki, T. Kawaguchi, M. Matoba, and H. M. Sen Gupta, Phys. Rev. C **70**, 034612 (2004).
[42] R. C. Diehl *et al.*, Phys. Rev. C **1**, 2132 (1970).
[43] A. Volya and V. Zelevinsky, Phys. Rev. Lett. **94**, 052501 (2005).
[44] D. H. Gloeckner, Nucl. Phys. A **253**, 301 (1975).
[45] C. M. Lederer *et al.*, Nucl. Phys. A **169**, 489 (1971).
[46] W. Booth *et al.*, Phys. Lett. B **30**, 335 (1969).